

# SPEKTRUM

Mitteilungsblatt der Fachgruppe Spektroskopie  
in der Vereinigung der Sternfreunde e.V.

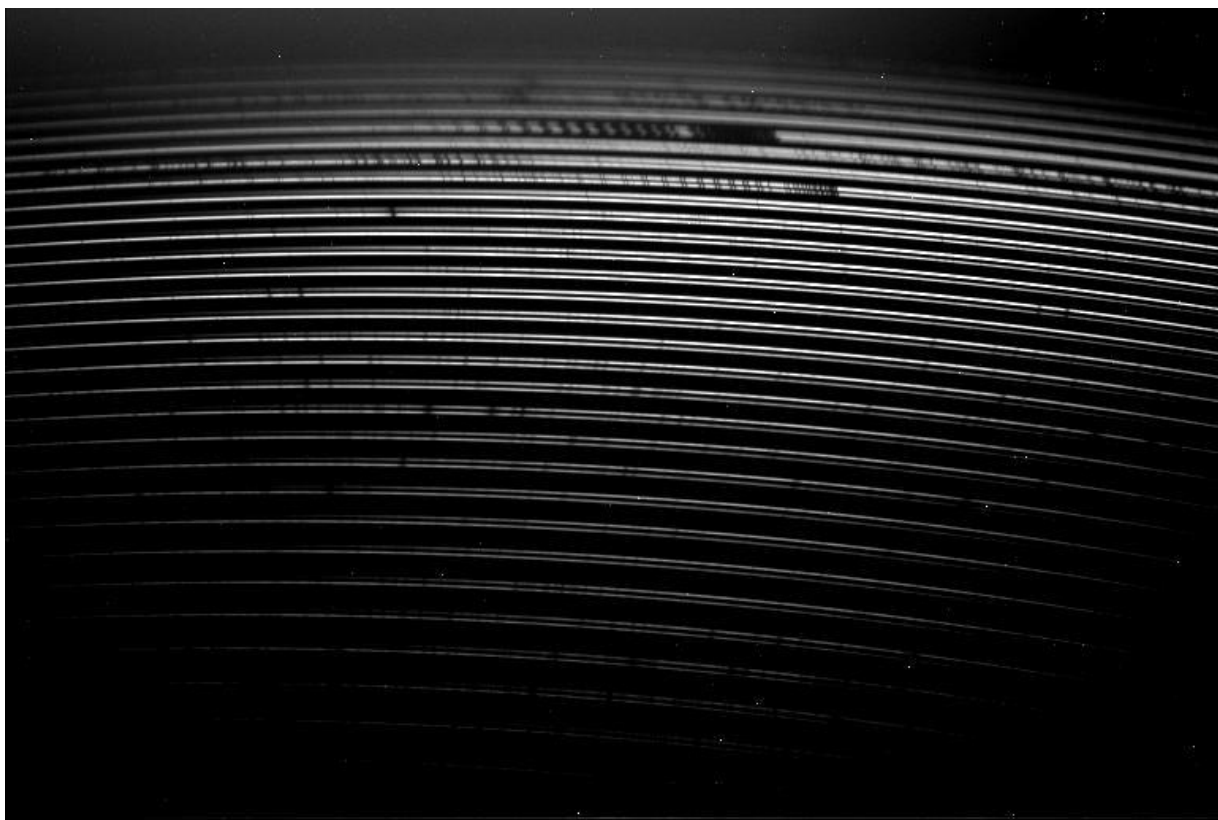
---

**NR. 46**

**INTERNETAUSGABE**

**1 / 2014**

---



**$\chi$  CYGNI MIT STARANALYSER 100**

**$\zeta$  PUPPIS PRO-AM CAMPAIGN PROPOSAL**

**FLISES**

**Spektrum – Mitteilungsblatt der Fachgruppe Spektroskopie in der Vereinigung der Sternfreunde** wird herausgegeben von der Fachgruppe Spektroskopie in der Vereinigung der Sternfreunde e.V. Es erscheint halbjährlich als PDF-Ausgabe oder auf Wunsch als Druckversion. Das Journal dient dem überregionalem als auch dem internationalen Erfahrungsaustausch auf dem Gebiet der Astropektroskopie besonders für Amateure. Dazu können Beiträge in Deutsch oder English publiziert werden. Senden Sie Ihre Beiträge, Auswertungen, Erfahrungen und Kritiken an **Spektrum** zur Veröffentlichung ein, damit andere Spektroskopiefreunde an Ihren Erkenntnissen teilhaben und davon lernen können.

**Spektrum – Mitteilungsblatt der Fachgruppe Spektroskopie in der Vereinigung der Sternfreunde** is issued twice a year by Fachgruppe Spektroskopie of Vereinigung der Sternfreunde e.V. (spectroscopy section of the German society for amateur astronomy). The journal is published as a PDF or as a printed version on special request. The aim of the journal is to be a national and international communication especially for amateurs, on topics related to astronomical spectroscopy. Contributions are welcome in German or English. Please send your papers, results, experiences and reviews to **Spektrum** for publication. The community can then benefit from your experience.

Registriert bei der Deutschen Nationalbibliothek / Registered at Deutsche Nationalbibliothek: DNB 1013413024

Die Fachgruppe Spektroskopie im Internet:

[spektroskopie.fg-vds.de](http://spektroskopie.fg-vds.de)

Die Vereinigung der Sternfreunde e.V. im Internet:

[www.vds-astro.de](http://www.vds-astro.de)

### Kontaktadresse (Redaktion, Bestellung gedruckter Ausgaben, Einsendung von Manuskripten)

Dr. Thomas Hunger  
Normannenweg 39  
D-59519 Möhnesee-Körbecke  
[thunger03@web.de](mailto:thunger03@web.de)

#### Hinweise für Autoren:

Nur durch Ihre Artikel wird Spektrum gefüllt. Die Redaktion behält sich vor, in Rücksprache mit den Autoren Beiträge zu kürzen, anzupassen oder zu ändern. Für die Inhalte der Artikel ist aber allein der Autor verantwortlich. Mit der Einreichung eines Beitrages erklärt der/die Autor(en) die Bereitschaft zur Publikation auch im Journal für Astronomie der VdS e.V.

Reichen sie Ihren Beitrag bitte elektronisch unter Berücksichtigung folgender Regeln ein:

Form des Textes: Senden sie vorzugsweise als unformatierten ASCII-Text. Tabellen mit Tabulatoren getrennt. Ein zusätzliches PDF des formatierten Gesamttextes ist anzuraten.

Aufbau der Artikel: Die Artikel benötigen einen Titel, eine vollständige Adressangabe des Autors / der Autoren, eine Kurzzusammenfassung, den klar gegliederten Artikel mit Einleitung und Zusammenfassung sowie eine vollständige Literaturangabe.

Abbildungen: Bitte trennt vom Text senden. Empfehlenswert sind hochauflösende JPG, PNG und TIFF.

#### Hints for authors:

Your article will be edited to fit the style of Spektrum. The editor is responsible for editing the article in close collaboration with the author. The author is in charge of the content in all cases, however. The author(s) express(es) the permission for a further publication of the contribution in the journal of the VdS e.V. (Journal für Astronomie) right with its transfer to the editor of Spektrum. Please send your contribution via electronic mail considering the following rules:

Text: Prepare it as unformatted text (preferably ASCII). Tables: columns separated by tabs. A PDF printout of the whole document is highly recommended.

Article structure: Each article should include a title, an address line of the author(s), an abstract, a clear text body with introduction and conclusion and complete references.

Figures: Please send them separate from text. High resolution JPG, PNG or TIFF files are recommended.

Beiträge sind urheberrechtlich geschützt. Alle Rechte sind vorbehalten. Autorenbeiträge, die als solche gekennzeichnet sind, stellen nicht in jedem Falle die Meinung des Herausgebers oder der Redaktion dar. Beiträge in dieser Ausgabe dürfen nicht ohne Genehmigung der Redaktion bzw. des Sprechers der Fachgruppe Spektroskopie in der VdS e.V. nachgedruckt, kopiert oder anderweitig weiterverwendet werden.

---

Umschlagfoto: Sonnenspektrum aufgenommen mit FLISES. Mehr dazu im Artikel von Daniel Sablowski im Heft.

# Inhaltsverzeichnis / Content

*Torsten Hansen:*

Beobachtungen des langperiodischen Veränderlichen  $\chi$  Cygni nahe seines Maximums mit Staranalyser 100 und Videokamera

**4**

*Tony Moffat and Thomas Eversberg:*

Getting to the Bottom of Co-rotating Interaction Regions in Luminous Hot Stars:  
A Pro-Am Campaign on the Southern O-type Super-giant  $\zeta$  Puppis

**6**

*Daniel Sablowski:*

FLISES – Fiber-Linked Image-Sliced Echelle-Spectrograph

**10**

*Thomas Eversberg and Klaus Vollmann:*

Fiber Noise and Photometric Shift

**14**

Termine

**18**

Mitgliederverzeichnis (nur Mitglieder) / Register of members (members only)

**19**



## Editorial

Liebe Leser des Spektrums,  
liebe Fachgruppenmitglieder,

eine echte Premiere für mich als Herausgeber: die erste Ausgabe von Spektrum im neuen Jahr ist vor der ASpekt verfügbar. Das ist natürlich nur dank der Autoren möglich, die frühzeitig Artikel eingesandt haben. Eine lobenswerte Leistung!

Apropos ASpekt: Die Vorbereitungen laufen auf Hochtouren, ein vollgepacktes und erstklassiges Programm mit Vorträgen von spektroskopischen Anfängern bis zum Profi erwartet die Teilnehmer. Dazu die Möglichkeit, persönliche Kontakte zu knüpfen und zu pflegen. Wer sich noch nicht zu einer Teilnahme entschieden hat: auf nach Köln.

In dieser Ausgabe von Spektrum gibt es kleine kosmetische Retuschen am Layout. Zu jedem Artikel wurde die Information zum Eingang des Papiers, der Revision und schließlich der Annahme eingefügt. Für die kommende Ausgabe plane ich die Einführung einer Letter-Sektion. Dort werden Kurzartikel ihren Platz finden.

Verbleibt noch: Viel Spaß beim Lesen!  
Mit sternenfreundlichen Grüßen,  
Ihr Thomas Hunger

Dear readers of Spektrum,  
dear members of the section,

A real premiere for me as the editor: the first annual issue of Spektrum is published before ASpekt will take place. Of course, this is possible only by the early submission of papers by the authors. A laudable achievement!

Speaking of ASpekt: Preparations are in full progress, a packed first-class program of lecture notes given by spectroscopic beginners up to professionals is waiting for the participants. Finally, don't miss the opportunity to create and maintain personal contacts. To all who didn't decide to participate yet: Go to Cologne.

In this issue of Spektrum there are minor cosmetic touch-ups regarding the layout. For each article an information about the original receipt, the revision and finally of the acceptance is now available. For the next issues I plan to introduce a Letter section. There, short articles will find their dedicated place.

Last not least: Have much fun reading!  
Clear skies.  
Yours Thomas Hunger

# Beobachtungen des langperiodischen Veränderlichen $\chi$ Cygni nahe seines Maximums mit Staranalyser 100 und Videokamera

Torsten Hansen

Reichau 216, 87737 Boos, Germany, Email: to.hansen@yahoo.de

## Zusammenfassung

2013 war spektroskopisch ein recht interessantes Jahr, auch für niederauflösende Spektroskopie, wie etwa mit dem Staranalyser 100. Der folgende Beitrag gibt ein Beispiel im Sinne einer allgemeinen didaktischen Herangehensweise an die Spektroskopie (durchaus auch noch aus Anfängersicht), unter Zuhilfenahme eines ausgereiften Instrumentariums (stabile Nachführung mit parallaktischer Montierung, Spiegelteleskop, Videokamera).

## Abstract

2013 was a quite interesting year for spectroscopy even with low dispersion as with the Staranalyser 100. The following report presents an example in terms of a general didactical approach to spectroscopy (from a beginner's view point too) with the help of a mature equipment (stable tracking with equatorial mount, reflector telescope, video camera).

Received: 2014-01-06, Revised: 2014-04-16, Accepted: 2014-05-02

Der interessante langperiodische Veränderliche  $\chi$  Cygni erreichte Anfang Mai 2013 seine maximale Helligkeit mit visuell angenehmen ca. 3,9 mag (Abb. 1). Diese Gelegenheit sollte genutzt werden, endlich auch einmal das Schmidt-Cassegrain-Teleskop mit 125 mm Öffnung und den Alan-Gee-Telekompressor auf seine spektroskopische Tauglichkeit hin zu testen.



Abb. 1: Sternfeld um  $\chi$  Cyg. Aufnahmedaten: 9 cm f/4,5 Refraktor, Canon 450D, 5 x 90 s, ISO800, 5.5.2013, 23:40-23:52 UT.

Da der Autor von dem Stern außer dem Spektraltyp S6 eigentlich nichts weiter wusste, war diese Beobachtung also auch auf Überraschungen angelegt. Dies machte den Reiz der Anwendung des Staranalyser 100 aus, auch gerade im Sinne eines entdeckenden Herangehens an die Spektroskopie, dass man auf sehr einfache Art ein unmittelbar befriedigendes Erlebnis hat.

So war es auch in diesem Fall. Der erste Blick im Livebild der Videokamera offenbarte bereits

die typischen kräftigen Banden eines Sterns späten Typs. Bei einer früheren Beobachtung von Mira ( $\alpha$  Ceti) nahe des Maximums waren damals im Livebild Emissionslinien im Blauen zu sehen gewesen. Interessanterweise waren diese auch bei diesem Stern sichtbar. Trotz nur durchschnittlichem Seeing waren schon im Livebild am blauen Ende des Spektrums zwei deutlich abgesetzte helle Punkte sichtbar (Abb. 2)!



Abb. 2: Rohspektrum von  $\chi$  Cyg mit Emissionslinien (markiert mit Pfeilen) im blauen Ende des Spektrums (links).

Laut Gray und Corbally, Ref. 1, zeigt Mira nahe ihres Maximums Emissionen bei den Wasserstofflinien  $H\gamma$  und  $H\delta$ . Dieselbe Quelle weist  $\chi$  Cygni ebenfalls als Mira-Typ aus. Bei Gray und Corbally sind noch weitere, höher aufgelöste Spektren von S-Sternen zu finden, die  $H\gamma$  und  $H\delta$  deutlich in Emission zeigen.

Für den Nachweis der Emissionen (angesichts der niedrigen Auflösung des Staranalyser 100) hängt bei der Auswertung, ähnlich wie damals bei Mira, manches an der Interpretation des Beobachters. So ist in Abb. 3 die Liniendarstellung des Spektrums (Graphik 3 und 4) natürlich abhängig von der Wahl des Kontinuums (violetter Graph mit Bezeichnung „continuum graph of spectrum Chi Cyg“ in Graphik 2 und 3).

Da aber die beiden Emissionslinien im Zusammenhang mit der Wellenlängenkalibrierung gewissermaßen "an der richtigen Stelle sitzen", sollte es sich um reale Details handeln. Absorptionslinien sind gemäß der Spektren in Ref. 1 blau-seitig nicht zu erwarten.

Später gelangen noch einige Folgebeobachtungen des Sterns, über die sich der geneigte Leser noch im Internet auf astronomie.de informieren mag [2].

## Verweise

- [1] Stellar Spectral Classification; Richard O. Gray and Christopher J. Corbally; Princeton University Press; Princeton and Oxford; 1. Aufl. 2009
- [2] [http://forum.astronomie.de/phpapps/ubbthreads/ubbthreads.php/topics/1007629/Chi\\_Cygni\\_mit\\_Staranalyser100\\_#Post1007629](http://forum.astronomie.de/phpapps/ubbthreads/ubbthreads.php/topics/1007629/Chi_Cygni_mit_Staranalyser100_#Post1007629)

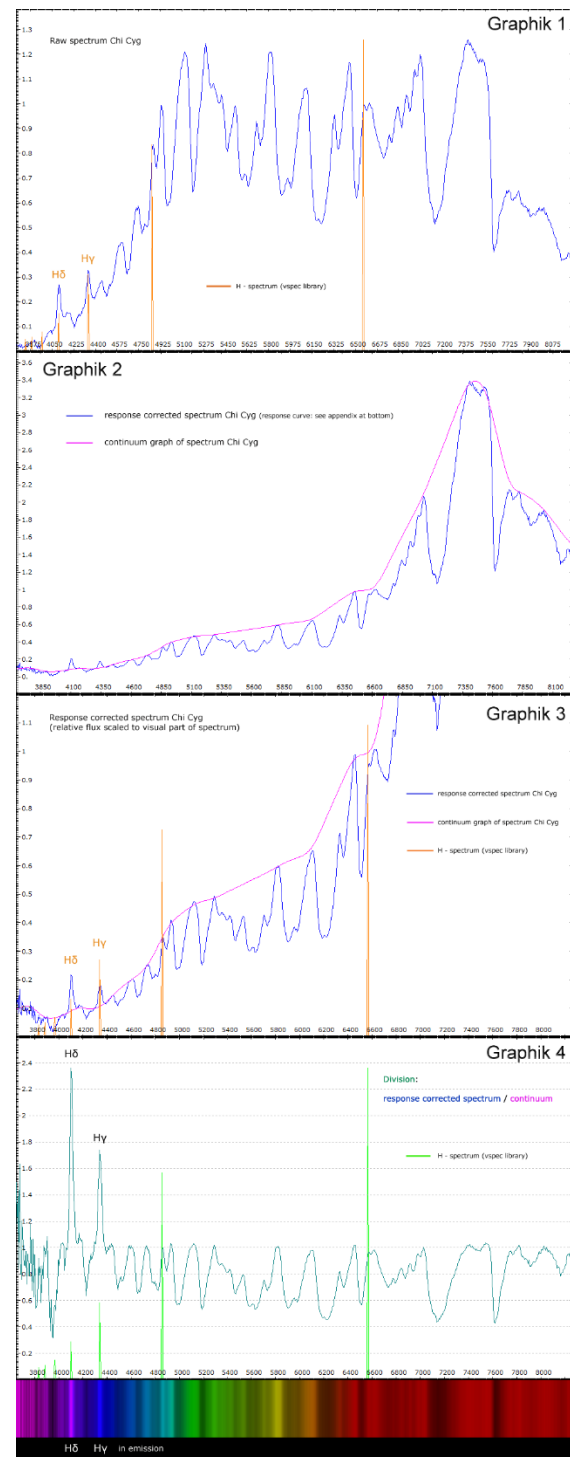


**Abb. 3:** Auswertung Spektrum  $\chi$  Cygni vom 06.05.2013. Rohspektrum (Graphik1); Instrumentenkorrektur und Kontinuumsfit (Graphik 2 und 3); auf Kontinuum normiertes Spektrum (Graphik 4); als Referenz sind den Graphiken Wasserstoff-Spektren unterlegt.

# Getting to the Bottom of Co-rotating Interaction Regions in Luminous Hot Stars: A Pro-Am Campaign on the Southern O-type Supergiant $\zeta$ Puppis

**Tony Moffat\*** and **Thomas Eversberg<sup>†</sup>**

\* Université de Montréal, Canada; Email: moffat@astro.umontreal.ca

<sup>†</sup> Schnörringen Telescope Science Institute, 51545 Waldbröl, Germany; Email: thomas.eversberg@stsci.de

## Abstract

Massive stars are the main source of ecological evolution in the Universe. Key elements of these stars are their very strong winds, whose properties we need to intimately understand. One complication in the winds of massive stars are recurring structures, which are a common, if not inherent phenomenon. One type of structure known for over two decades are large-scale spiral-shaped Co-rotating Interaction Regions (CIRs), which manifest themselves in spectral line variations (ref. [1]). Although previous measurements have confirmed the basic idea of these structures, spectroscopic observations over longer time scales to determine the physical causes are still lacking. Are the structures permanent or temporary? What is the production mechanism at the stellar surface? We want to answer these key questions for  $\zeta$  Puppis, the brightest and hottest O supergiant in the sky. With magnitude V = 2.25 mag, high quality repeated spectra can be obtained even with very small telescopes. This should be accompanied by high-precision photometric monitoring, which is most sensitive to continuum emission from bright spots at the stellar surface giving rise to the CIRs.  $\zeta$  Puppis is a star in the southern hemisphere and thus an attractive target not only from a physical point of view but also well suited to motivate potential observers in the south to provide professional spectroscopic data.

## Zusammenfassung

Massereiche Sterne sind die Hauptquelle der ökologischen Entwicklung im Universum. Schlüsselemente dieser Sterne sind ihre sehr starken Winde, deren Eigenschaften wir verstehen müssen. Eine Komplikation in den Winden massereicher Sterne sind wiederkehrende Strukturen, die ein übliches, wenn nicht inhärentes Phänomen darstellen. Eine dieser seit über zwei Dekaden bekannten Strukturen sind spiralförmige rotierende Regionen (Co-Rotating Interaction Regions - CIR), die sich in Variationen von Spektrallinien manifestieren [1]. Obwohl frühere Beobachtungen die Grundvorstellung von diesen Strukturen bestätigt haben, fehlen spektroskopische Messungen über längere Zeitskalen, um die physikalischen Ursachen zu bestimmen. Erscheinen die Strukturen permanent oder temporär? Was ist der ursächliche Mechanismus an der Sternoberfläche? Wir wollen diese Fragen für  $\zeta$  Puppis beantworten, dem hellsten und heißesten O-Riesen am Himmel. Mit seiner scheinbaren Helligkeit von V = 2,25 mag, können auch mit sehr kleinen Teleskopen wiederholt Spektren hoher Qualität gewonnen werden. Dies sollte durch eine hochpräzise photometrische Überwachung begleitet werden, die am empfindlichsten auf Kontinuumsemissionen von hellen Flecken (die mögliche Ursache von CIRs) an der Sternoberfläche reagiert.  $\zeta$  Puppis ist ein Star in der südlichen Hemisphäre und damit ein attraktives Ziel nicht nur aus physikalischer Sicht, sondern auch gut geeignet, um potentielle Beobachter im Süden zu motivieren professionelle spektroskopische Daten zu gewinnen.

Received: 2013-12-26, Revised: 2014-04-16, Accepted: 2014-05-02

## 1. Preamble

A single luminous and massive hot star can reach up to over a million times brighter than the Sun, with most of its radiation emitted in the ultraviolet (UV), in contrast with the Sun's peak intensity in the visible part of the spectrum. Such massive stars are renowned for their dominating effect on the ecology of the cosmos. They enrich the interstellar medium (ISM) with progressively richer nuclear-processed matter during their whole lifetimes via strong stellar winds,

culminating as supernovae. The ejection process also feeds huge amounts of energy into the ISM, both from the ionizing effect of photons and from the kinematics of rapidly expelled matter.

It is now firmly established that virtually all luminous hot O-type stars reveal Discrete Absorption Components (DACs) in their spectra – see Fig.1.

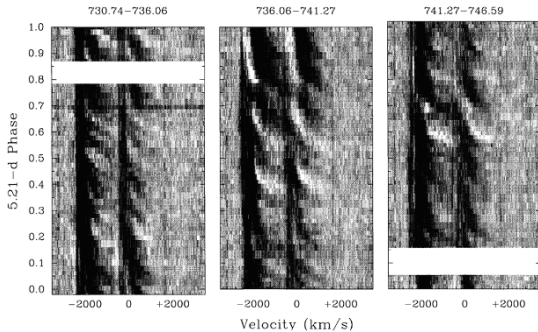


**Fig. 1:** Illustration of typical DACs in hot luminous stars from UV-spectroscopic observations of the bright early-O supergiant  $\zeta$  Pup from a single 16-day run with the International Ultraviolet Explorer satellite (IUE) after rationing with a template minimum-absorption spectrum of the unsaturated P Cygni resonance line pair Si IV 1394/1403A. The velocity scale refers to Si IV1394; that for Si IV1403 can be easily derived from this. The wind terminal speed is  $\sim 2500$  km/s. The whole run is broken up into three nearly equal parts, each covering a rotation cycle of 5.21 days. This reveals a large number of moving excess absorption troughs (the curved black streaks, typically  $\sim 6$ ) [2]. While DACs are always present, they do not repeat for more than a couple of rotations.

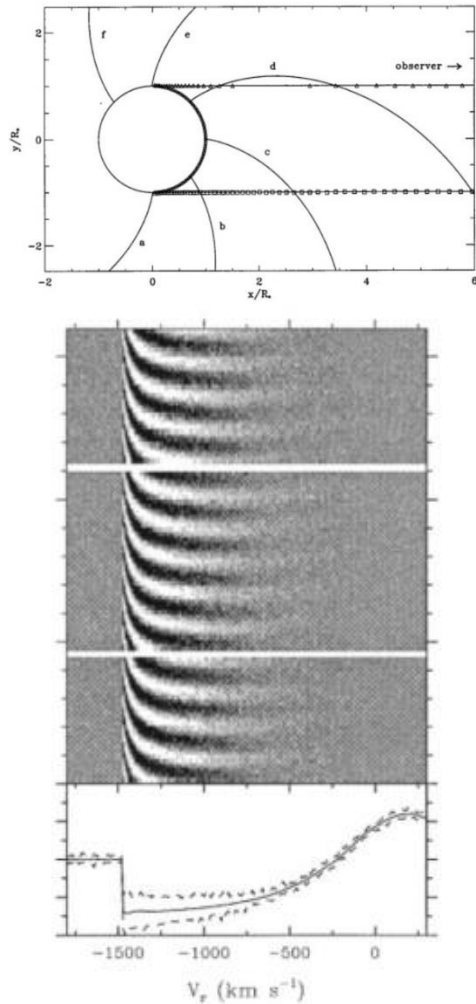


**Fig. 2:** Top: Crossing of co-rotating shock patterns along the line-of-sight absorption column. Bottom: Gray-scale representation of the spectral flux variations for a marginally optically thick single line formed in a wind model with co-rotating density enhancements induced by non-radial pulsations in an O-type star [4].

These are excess absorption components seen in the absorption edges of P Cygni lines mostly in the UV, where wind-lines are best seen. These absorption components start out shallow and broad, becoming deep and wide as the wind terminal speed is approached (depending on the strength and degree of saturation of the line). The best interpretation of DACs is the model for co-rotating interaction regions (CIRs) by Cranmer & Owocki [3] in which a bright rotating spot on the surface of the star imposes a perturbation in the wind, leading to a co-rotating spiral-shaped shock-wave whose material propagates outward in the wind and is seen as a DAC in the absorption component of a P Cygni spectral line – see figs. 2 and 3.

While non-radial pulsations (NRPs) were originally thought to be the best candidate for creating bright spots, the preferred mechanism now appears to be magnetic bright spots [5], now inspired by the recent revelation of a sub-surface convection zone that can create such spots [6]. Perhaps both mechanisms are operating, although NRPs will tend to be rotating either faster (prograde) or more slowly (retrograde) than the star, while magnetic spots will follow the stellar rotation. At first the bright spot blows a denser wind than average, but then as the star rotates, this higher-density sub-region finds itself above average regions of the star with less driving than it had at the beginning. This makes the sub-region slowing down in its expansion, thus plowing into the faster-expanding ambient wind and setting up a shock, which ultimately takes the form of a spiral as the star rotates. There could be any number of such spirals in the wind (as there are bright spots on the star), although normally only two dominating ones are seen per rotation cycle [7].

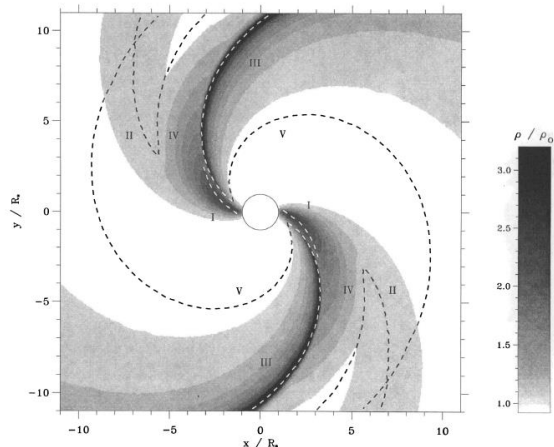


**Fig. 3:** Normalized density gray scale for CIR in the equatorial plane of an O star [3]. The drivers are two bright spots arbitrarily placed at diametrically opposite sides of the star.

But it still remains to be shown that such bright spots are present in any given O star and that

they actually do give rise to CIRs (and hence DACs). Recent monitoring of the northern O7.5III star  $\xi$  Per [8] with the MOST satellite shows that rotating bright spots with lifetimes of 2-3 rotations are indeed seen in the continuum light coming from the stellar photosphere. But simultaneous spectroscopy was not available for  $\xi$  Per to test for the connection between CIRs (e.g. DACs from UV or H $\alpha$  spectroscopy) and bright spots (continuum photometry).

## 2. Why $\zeta$ Puppis?

We propose to monitor the brightest early-type O star in the sky,  $\zeta$  Puppis, mainly in the line of He II 4686 Å, which shows a near-central absorption reversal superposed on a weak wind-emission line (as does H $\alpha$ , but He II 4686 is better to observe than H $\alpha$  because it is not inflicted with numerous telluric features).

This absorption reversal behaves like the P Cygni absorption edges seen in the UV, but even better, probes the inner wind just above the stellar surface where one can more easily link its variation to rotating bright spots in the photosphere of the star. The passage of a CIR across the line of sight will cause an enhancement in the depth of the absorption reversal; we may see several of them during a rotation cycle of 5.2 d [9] - supported by later observations [10] - who actually concentrated more on the lower-amplitude, small-scale clumps in the wind, which will not be considered in the present study.

In fact, the DAC timescales in the UV suggest that there may be as many as 6 CIRs passing across the line of sight per rotation cycle [2], although this is subject to evolve with time as more spots are expected to come and go over several rotation times, but always with the same rotation rate (within a small dispersion due to possible differential rotation from equator to pole) – see fig. 1. He II 4686 will probe the absorption properties of the passing CIRs in the inner wind. We will also examine the variable behavior of other nearby lines due to N V and N III, the latter further out in the wind. In order to correlate these spectral reversal variations of the CIR with bright (magnetic?) spots in the photosphere, simultaneous high-precision photometry is also needed.

## 2. Call for an observational campaign

We request moderately high-cadence spectroscopic observations of the He II 4686 Å line covering Jan – April 2014 with R ~ 5000, S/N ~ 500,

and over at least 4570 – 4740 Å, like that already obtained by B. Heathcote, see fig. 4. We also request quasi-simultaneous, high-cadence (at least as often as the spectra), high-precision (rms no worse than 3 mmag per data-point) dual-band (e.g. broadband B-R or similar; narrowband even better if centered mostly on the stellar continuum) differential photometry.

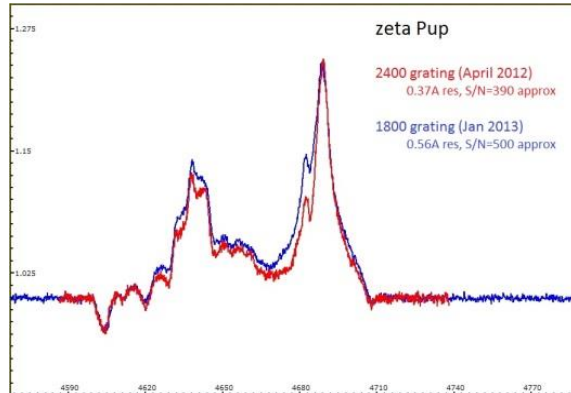


**Fig. 4:** Previous spectra of  $\zeta$  Pup obtained by B. Heathcote, of the kind needed in this proposal.

Ideally, we need at least 2-3 such spectroscopic observations spread out as much as possible during the night - over as many clear nights as possible - in order to determine the lifetime of each CIR (2-3 rotations?) and see how often and frequently the CIRs appear. We realize that differential ground-based high-precision photometry is difficult to achieve with such bright stars, which are generally rather sparsely dispersed over the sky for this technique to work well. However, it's worth a try. In any case, we may have another opportunity to carry out high-cadence precision photometry in a year or two from space using BRITE-Constellation [11], currently three nanosatellites, each equipped with 30 mm telescopes and one medium-band filter, either optical blue or red. This mission is currently still in commissioning phase with three more nanosatellites to join BRITE-Constellation in 2014. BRITE-Constellation will be available for regular observing by the middle of 2014 in pre-selected fields, too late for  $\zeta$  Pup in its best current observing season, early 2014. For now, it would be extremely useful to gather a large bank of time-resolved spectra, even with less precise ground-based photometry, to judge how things will pan out, i.e. do we see multiple CIRs of different strength, repeating on 2-3 times the rotation timescale? Is there any hint that bright spots appear in continuum photometry at the same time that CIRs appear at the base of the wind? Depending on the clarity of the outcome here, we may always have the option of follow-up in a future simultaneous run between ground-based spectroscopy and space photometry with BRITE-Constellation. All results will be published in any case.

**Appendix A Data of  $\zeta$  Pup**

$\zeta$  Puppis = zeta Pup = HD 66811  
Position: 08:03:35.05 -40:00:11.3 (2000)  
Brightness: V = 2.25, B = 1.97, U = 0.88  
Spectral type: O4If(n)p

- [4] Owocki et al., 1995, ApJ, 453L, 37
- [5] Henrichs, 2012, Publ. Obs. Astron. de Beograd, 91, 13
- [6] Cantiello et al., 2009, A&A, 499, 279
- [7] Kaper et al., 1999, A&A, 344, 231
- [8] Ramiaramanantsoa et al., 2014, submitted
- [9] Moffat & Michaud, 1981, ApJ, 251, 133
- [10] Eversberg et al., 1998, ApJ, 494, 799
- [11] <http://www.brite-constellation.at/>

**Literature**

- [1] Eversberg & Moffat, 2012 Spektrum, 42, 14
- [2] Howarth et al., 1995, ApJL 452, L65
- [3] Cranmer & Owocki, 1996, ApJ, 462, 469

# FLISES – Fiber-Linked Image-Sliced Echelle-Spectrograph

**Daniel Sablowski**

Erich-Weinert-Str. 19, 14478 Potsdam, Germany, Email: danielsablowski@gmail.com

**Abstract**

This article describes an Echelle spectrograph for high-precision measurements in the field of amateur spectroscopy. Echelle spectrographs are used in professional instrumentation since many years. However, amateurs use also some commercial available devices with good success. The spectrograph described here is enclosed in a thermally stabilized housing to achieve high precision in wavelength calibration. It is linked via a fiber-link to a 10 inch f/4 Newtonian telescope. The observatory is remotely controlled from a control room or via internet from all over the world. The spectrograph itself is placed in the telescope control room.

**Zusammenfassung**

Dieser Artikel beschreibt einen Echelle-Spektrographen für hoch-präzise Messungen im Felde der Amateurspektroskopie. Echelle-Spektrographen werden bereits seit vielen Jahren von professionellen Astronomen eingesetzt. Auch Amateure nutzen kommerzielle Echelle-Spektrographen mit Erfolg. Der hier beschriebene Spektrograph ist in einem thermisch stabilisierten Gehäuse untergebracht, um eine hohe Genauigkeit in der Wellenlängenkalibration zu erhalten. Er ist mittels Faserkopplung an ein 10" f/4-Newton-Teleskop gekoppelt. Die Sternwarte wird von einem Kontrollraum aus ferngesteuert, kann aber auch über das Internet von überall auf der Welt angesteuert werden. Der Spektrograph selbst ist im Kontrollraum untergebracht.

Received: 2014-02-17, Revised: -, Accepted: 2014-05-02

## 1. Introduction

Radial velocity (RV) measurements require high precision in wavelength calibration and, equally important, time-stable calibration. This makes it necessary to thermally control the spectrograph environment. The use of fibers to link the spectrograph to the telescope provides for a high mechanical stability. Nevertheless, fibers do not scramble the spatial information of the position of the star at fiber entrance perfectly, but do a much better job than a slit of a direct-linked spectrograph. The scrambling is in the case of FLISES not the main problem. It will be an issue when spectrographs with a resolving power of  $R > 30.000$  are used to get precisions down to some m/s.

An Echelle on the other hand, has a great advantage in the sense of measurement statistics: Many lines are simultaneously measured and are used to get better averaged values for wavelength shifts and line profiles. The standard procedure is to take calibration frames before and after the object exposure and use the averaged frame for calibrating the object spectra. However, in professional instrumentation a common way is to simultaneously expose both, object and calibration frame. This is done by generating two spectra, one of the calibration light and one of the object. This is realized by

placing two fibers in the focal plane of the spectrograph collimator. The calibration lamp intensity is adapted to the exposure time of the object spectra to avoid overexposing of the calibration spectra. It is also possible to shutter the calibration light in a suitable way. The calibration spectra now shows the shifts of the spectral lines due to instrumentally introduced deviations. It is not a big problem to implement such a calibration procedure to amateur sized spectrographs but it has never done before so far.

Capture 2 discusses the optical layout of the spectrograph, chapter 3 the fiber-link and the telescope. The thermally stabilized housing is discussed in chapter 4 and chapter 5 is reserved for results and efficiency discussion.

## 2. Optical Layout of FLISES

FLISES is based on a classical spectrograph design layout: slit, collimator, grating, cross-disperser, imaging optics and CCD. However, an Echelle grating with a size of 160 mm x 65 mm from a Perkin-Elmer lab-spectrograph is used. Therefore, a long focal-length collimator can be used to achieve high resolution. To increase the resolution furthermore, an image slicer [1] is implemented to cut the fiber into two pieces and hence increase the resolution by a factor of 2.

To cross-disperse the highly overlapping diffraction orders (illuminated by the Echelle grating) a dispersion prism made from F2 glass with an antireflection coating is used.

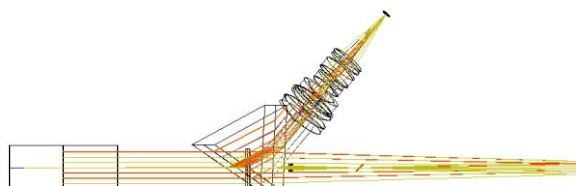


Fig. 1: FLISES Layout side view.

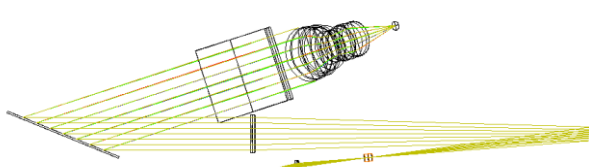


Fig. 2: FLISES Layout top view.

In fig. 1 the side view of the layout is shown. Left rectangle is the Echelle grating, followed by the prism and imaging optics. In the background of the prism, the collimator is visible.

The top view of the layout is shown in fig. 2. At the middle and bottom of the image, the fiber entrance is shown with transformation optics to feed the image slicer. The beam is then folded by a flat mirror and collimated by an achromatic doublet f/16 with  $f = 750$  mm. The Echelle (79 grooves/mm blazed at  $\Theta_B = 63.4^\circ$ ) diffracts the light to the prism and is imaged onto a CCD.

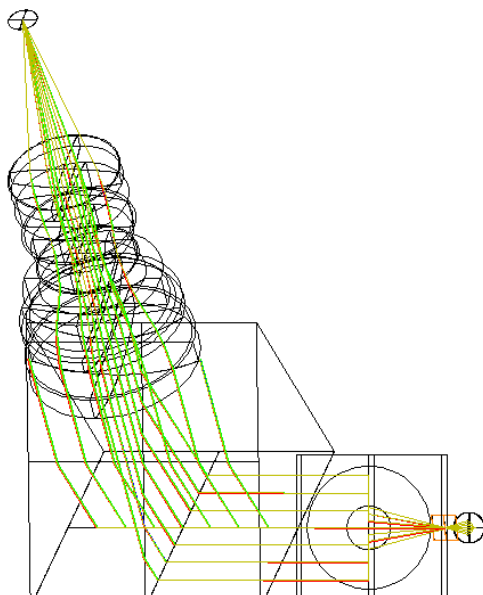


Fig. 3: FLISES Layout front view.

A Moravian G21600 with KAF1603ME and an active area of  $13.8 \times 9.2$  mm $^2$  as well as  $9 \times 9 \mu\text{m}^2$  pixel size was chosen as the detector. With such a small CCD a fast camera is necessary. This is the main problem of amateur instrumentation in that field. Luckily, there are some "standard" camera lenses which provide good imaging quality and can be used for that application. Nonetheless, one has to find such a lens in the crowded field of lenses. If a lens is found, success (a first spectra) is visible.

The Echelle grating is blazed to a specific angle, depending on the line density and the used wavelength range. The angle is, surprisingly, such that the rays following the law of reflection at the groove surface. That is why the grating should be used near the Littrow configuration (angle of incidence equals angle of diffraction). The total angle (angle between the incident and diffracted beam) is  $10^\circ$  in the case of FLISES. However, it is possible to reduce this angle to  $0^\circ$  by tilting the grating in the grating plane but this causes an inclination of the spectral lines.

The fiber provides an output of approx. f/4 and - to get better slicing conditions - the fiber is magnified by a factor of 4 onto the image slicer. Hence, the fiber image has a diameter of 200  $\mu\text{m}$  and surface imperfections of the slicer-plate are small compared to the fiber image. An image of the sliced fiber is shown in fig. 4.



Fig. 4: Image of the sliced fibre.

The f/4 beam is reduced to f/16, the focal length of the collimator was set to 750 mm and a diameter of 2" (750/16 mm  $\sim$  47 mm) is necessary. For a total angle of  $\psi = 10^\circ$  we get for the angle of diffraction

$$\beta = \Theta_B - \psi/2 = 58.4^\circ$$

and for the angle of incidence

$$\alpha = \Theta_B + \psi/2 = 68.4^\circ.$$

Because the angle of incidence is not equal the angle of diffraction (as it is for a mirror) the beam size  $w$  is converted to

$$w' = w a,$$

where  $a = \cos(\beta)/\cos(\alpha) \sim 1.42$ . The size of the slit  $b'$  in the image plane is then given by

$$b' = b \cdot a \cdot \frac{f_{lens}}{f_{coll}}$$

where  $b$  is the slit width,  $f_{lens}$  the focal length of the camera lens and  $f_{coll}$  the focal length of the collimator. With the values in the case of FLISES, we find  $b' \sim 20.7 \mu\text{m}$ . Remember the Nyquist criterion, which says that a function of frequency  $f$  must be measured with a frequency of  $2f$ . In the case of a spectrograph the measuring frequency are the periodic pixels on the CCD. The size is  $9 \mu\text{m}$  and  $b'$  must be imaged onto two pixels. This is fulfilled in the case of FLISES, because the scan-factor is  $u = b'/(2p) = 1.15 > 1$ , where  $p$  is the pixel size. Note that by a slit size of  $20.7 \mu\text{m}$  good imaging optics are necessary to get the geometric calculated resolution.

### 3. Fiber-link and FLISES' telescope

The fiber is a  $50 \mu\text{m}$  silica-silica broadband one useable for the visible range of the spectra. It is fed by a f/4 telescope in prime focus. At  $4''$  seeing the seeing disc has a FWHM of approx.  $20 \mu\text{m}$  and therefore a reflective pinhole with a diameter of  $50 \mu\text{m}$  is used and imaged onto the fiber. The reflective pinhole is used to guide the target star. Fig. 5 shows a star located on the pinhole, viewed from the guide cam of the telescope.



Fig. 5: Star on pinhole.

The imaging optics behind the pinhole are achromatic and aspherized to achieve smaller spot sizes. The magnification is unity because f/4 is already a good compromise between FRD and throughput.

The telescope is build out of rectangular steel tubes and the fiber injection is directly placed at the prime focus of the  $10''$  f/4 parabolic mirror. The mirror is supported by a 9 point mirror cell.

The telescope itself is supported by an automated Rupp mount which is controlled with the Little Foot Elegance Photo telescope step motor controller.



Fig. 6: Telescope.

### 4. Thermally stabilized housing

The housing has an outer wall, an isolating layer made from rigid foam and an inner wall. The CCD is placed inside the housing and hence, the heat produced by the electronics must dissipate out of the housing. To achieve this and to stabilize the temperature inside the box, a Peltier cooling system is used. It consists of a Peltier element between two heat sinks which are cooled by fans. A temperature sensor is placed inside the box to control the temperature automatically by a temperature control unit via PID-control. The deviation in temperature is  $\pm 0.2^\circ\text{C}$ .

### 5. Results

Because the efficiency of the fiber link was measured in the laboratory to 75 % the losses in the fiber can be neglected (a part of these losses are already considered in the aforementioned measurement). The optical camera suffers from a strong focal shift to the red region (fig. 7) of the spectra, which could not be completely eliminated by adjusting the CCD independent from the camera. But the loss of resolution is far in the red and hence not critical for most measurements.

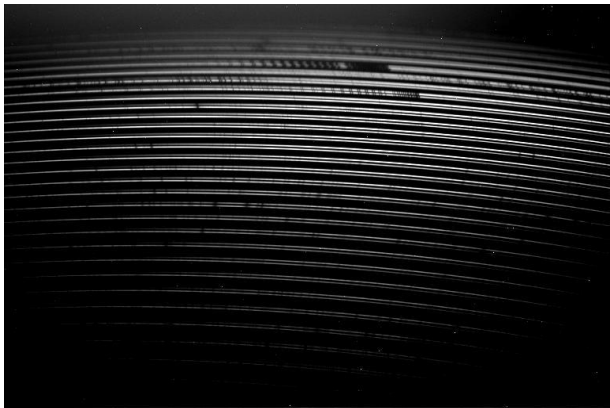


Fig. 7: Solar spectrum.

## 6. Conclusion

The fact that the limiting magnitude depends also on the size of the telescope, it is worse not-

ing, that frontier science is limited to professional astronomers. However, it is always possible to study fundamental stellar physics by observing bright stars. Often, stars, which we thought to understand, show strange changes and are still interesting to observe. By using very big telescopes, professionals are no longer able to study bright stars, because the detectors get overexposed! On the other hand, there are very interesting stars which are bright enough to be observed by amateurs and that's why it makes sense to construct such instruments.

## References

- [1] Daniel Sablowski, Simple Image Slicer, Spektrum – Mitteilungsblatt der Fachgruppe Spektroskopie, 43, 2/2012, 14ff

# Fiber Noise and Photometric Shift

**Thomas Eversberg and Klaus Vollmann**

Schnöringen Telescope Science Institute, 51545 Waldbröl ,Germany, [www.stsci.de](http://www.stsci.de),  
Email: thomas.eversberg@stsci.de

## Abstract

When a spectrograph or any other measuring system is positioned and fixed at the telescope focus we add additional masses, and both the optical and the mechanical behavior of the optical system is changed. This also applies to the bending behavior (i.e. flexure) of the spectrograph with respect to the telescope guiding and positioning. In short - additional masses disturb both the static and dynamic behavior of the entire measurement system. This can be compensated for by a mechanical reinforcement of all parts. However, strengthening in turn leads to more stress and deflection, which may eventually exceed the mechanical system boundaries. Telescope movements and resulting mechanical stress in the spectrograph in turn lead to spectral shifts that potentially affect the measurements. In addition, temperature and humidity fluctuations can also cause spectral shifts. Hence, it might be useful to disconnect the instrument from the telescope and run it in a different local environment. Instead of flanging the instrument to the telescope, fiber optics can transmit light from the telescope focus to the spectrograph, which can be placed in a stable, fixed position away from the telescope. Besides circumnavigating the above problems, fiber optics have even more advantages. The observer can be almost completely independent of the telescope and the spectrograph is not subject to weight or volume limits. This includes using techniques to achieve very high spectroscopic temperature stability and thus avoiding corresponding spectral shifts. However, there are prices to pay for the above advantages. Two of them are fiber noise and photometric shift.

## Zusammenfassung

Wenn ein Spektrograph oder ein anderes Messsystem im Teleskopfokus positioniert und fixiert wird, werden zusätzliche Massen hinzugefügt. Sowohl die optischen als auch die mechanischen Eigenschaften des optischen Systems werden verändert. Dies wirkt sich auch auf das Biegeverhalten des Spektrographen bezüglich Teleskopnachführung und Positionierung aus. Kurzum - Zusatzmassen stören sowohl das statische als auch das dynamische Verhalten des gesamten Messsystems. Dies kann durch eine mechanische Verstärkung aller Teile kompensiert werden. Allerdings führen solche Verstärkungen wiederum zu mehr Stress und Durchbiegungen, welche schließlich die mechanischen Systemgrenzen überschreiten können. Teleskopbewegungen und daraus resultierende mechanische Spannung im Spektrographen führen wiederum zu spektralen Verschiebungen, die potentiell Auswirkungen auf die Messungen haben. Zusätzlich führen Temperatur- und Feuchtigkeitsschwankungen zu spektralen Verschiebungen. Daher kann es sinnvoll sein, das Messinstrument vom Teleskop zu trennen und in einer anderen Umgebung zu betreiben. Anstatt das Instrument direkt am Teleskop zu befestigen, kann das fokale Licht mittels Faseroptik zum Spektrographen übertragen werden, der in einer stabilen Position getrennt vom Teleskop platziert werden kann. Neben der Vermeidung obiger Probleme haben Glasfasern noch mehr Vorteile. Der Beobachter ist beinahe vollständig unabhängig vom Teleskop und der Spektrograph unterliegt keinen Gewichts- oder Volumengrenzen. Dies beinhaltet die Nutzung von speziellen Techniken, um bei sehr hoher Temperaturstabilität entsprechend genaue spektroskopische Messgenauigkeiten zu erreichen und damit entsprechende spektrale Verschiebungen zu vermeiden. Allerdings zahlt man einen gewissen Preis für die oben genannten Vorteile. Zwei von ihnen sind Faserrauschen und photometrische Verschiebung.

This text is an excerpt from the text book "Spectroscopic Instrumentation – Fundamentals and Guidelines for Astronomers" to be published by Springer Verlag, 2014.

Received: 2014-03-05, Revised: 2014-04-16, Accepted: 2014-05-02

## 1. Fiber noise

A well-defined monochromatic beam introduced into a thin fiber is repeatedly reflected on its way through the fiber. Its intensity distribution at the

fiber end is not uniform but exhibits "discrete" maxima (speckles), spread stochastically over the fiber aperture (figure 1).

This is due to the many reflections of light rays within the non-perfect fiber as well as scattering at the entrance aperture and the resulting random reflection effects. The resulting thousands of rays introduced by different path lengths are called modes. Modes are produced by interfering light paths. They provide a structured light distribution at the fiber output. Blue light suffers more reflections than red light, thus generating a greater number of modes<sup>1</sup>. The emergence of modes is not an effect of Focal Ratio Degradation (FRD): modes are also formed in fiber optics which are not subjected to any stress. However, their distribution reacts highly sensitively to the smallest deformations or changes in position far below stress levels where FRD occurs. The motion of a telescope that feeds light to a spectrograph via fibers causes time-variable fiber modes. In practice they are inevitable. The reason is the illuminated entrance aperture of the fiber and its small irregularities, unavoidable even for a meticulously polished surface (figure 2).

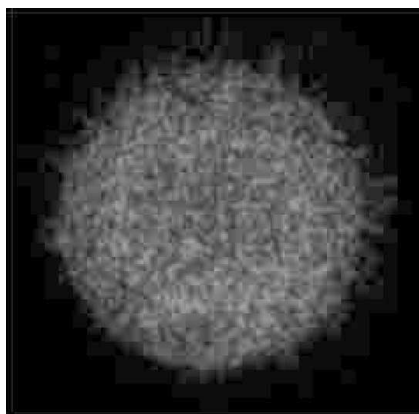


**Fig. 1:** Speckle distribution of monochromatic light of a 660nm-HeNe laser at the end of an optical fiber [1].

Each sub-region of the entrance surface is a source of scattered light rays. Depending on the surface roughness and the wavelength, the phase differences between individual modes can be up to several thousand radians. Therefore, the field intensity at each observation point P is determined by the mutual interference of a large number of wavelets that are coherent but not in phase when leaving the fiber. Stochastic effects from interference minima and maxima are inevitable at the fiber exit. If the observer moves to another place P, the path lengths of the scattered rays change and a new intensity distribution is introduced. The result is a far-field distribution of bright (constructive interference) and dark (destructive interference) spots. It

could now be argued that the speckles disappear behind an imaging lens if the rays of a small area can be appropriately mapped. But that is not the case, since we cannot correspondingly image all rays even with a very large lens (figure 3).

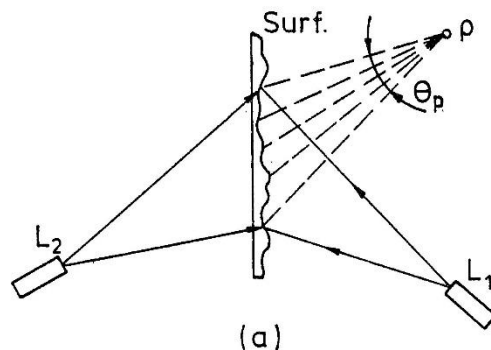


**Fig. 2:** Setup for the observation of fiber speckles in the far field [2].

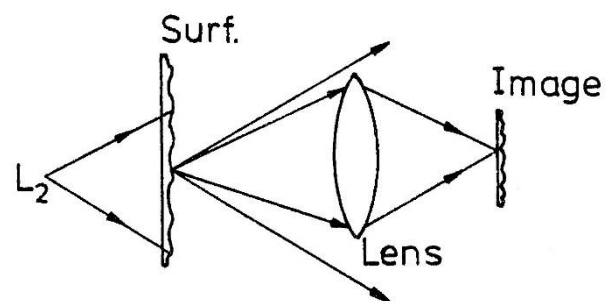


**Fig. 3:** Setup for the observation of fiber speckles by an imaging lens. The lens cannot image all rays of phase space [2].

Any finite aperture, even if it is perfect, provides only a portion of all phase information and therefore produces abrupt intensity changes in the image. Because of their stochastic nature in time (telescope movement) fiber modes are an additional source of noise. Completely analogous to the stochastic seeing of the night sky, the light at the fiber end is not uniform, but rather shows an intrinsic fiber noise over the entire aperture. The beams exit the fiber at different geometrical positions in time and are then vigneted stochastically during exposure through the optical slit. Therefore, for a given apparatus the attainable theoretical signal-to-noise ratio is significantly reduced. The number of modes at the fiber end depends on both the *F*-number at the fiber input and the wavelength. The bigger the input *F*-number (more reflections) and the

<sup>1</sup> The color-dependent transit time differences additionally introduce a reduction of signal quality and reduced bandwidth (modal dispersion). This can be

avoided by the use of gradient-index fibers. Their fiber core has continuous refractive indices decreasing towards the cladding. However, these effects can be neglected in astronomical spectroscopy.

shorter the wavelength, the more modes that develop in the fiber. Since the total light flux remains constant, few modes have a stronger effect on the S/N than many modes. As the number of modes at red wavelengths is much smaller than at blue wavelengths, one observes especially for longer wavelengths a significant reduction of the theoretically achievable S/N. In addition, one must keep in mind that the intensity fluctuations that produce the modes together with the vignetting slit, are greater the more the slit is vignetting. That is, especially at high resolution, achieved with a narrow slit, is fiber noise increased. Figure 4 shows a measurement result obtained with the FOCES spectrograph at Calar Alto Observatory. At red wavelengths the measured S/N is reduced by a factor of 2.5 compared to theoretical photon statistics.

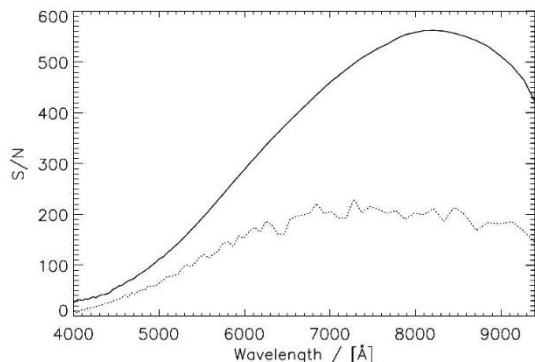


**Fig. 4:** Full line - Theoretical S/N according to photon statistics for the FOCES spectrograph. Dotted line – The measured S/N[1].

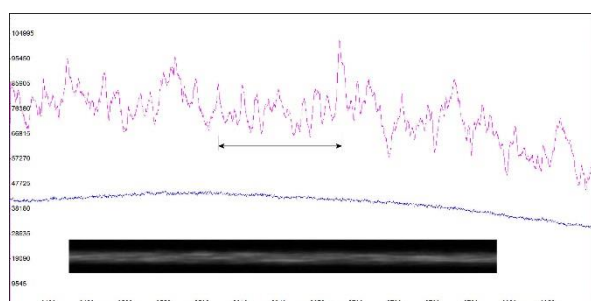


**Fig. 5:** "Shaking out" fiber modes. Top: Spectrum of a continuous tungsten lamp fed into a spectrograph with a 50 micron step-index fiber of 2m length. A 30 micron slit is positioned at the fiber entry to enhance the effect by stopping modes of large input angles. Bottom: 2D image of the top spectrum. The respective wavelength interval is indicated. Middle: Same as top but now with shaking the fiber during exposure. Note: The latter is obtained with a 20 micron slit again enhancing any mode effect. Even with lower entry angles the modes are entirely eliminated [3].

To minimize this massively disturbing effect and achieve maximum S/N in high-resolution spectroscopy mode, it is obvious to artificially generate as many modes as possible, which have an adequate distribution during exposure time and

thus ensure minimal fluctuations due to slit vignetting. This is done by non-harmonic motions of the fiber during recording. Amazingly, one can "shake out" the modes by hand. Even better, though, is an apparatus that produces non-harmonic motion of the fiber (for example, double-pendulum) to provide a stochastic distribution of the modes. This is shown in figure 5 for the light of a tungsten lamp.

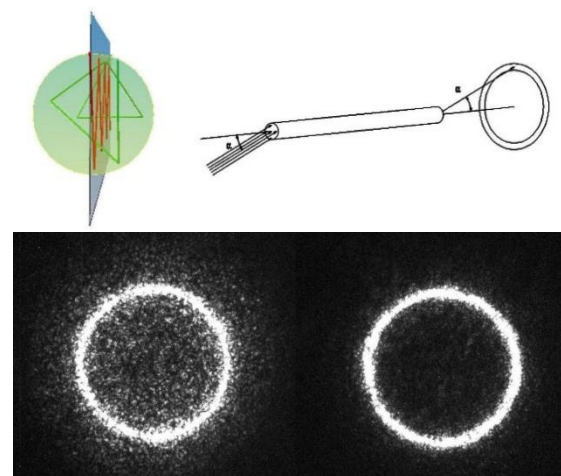


**Fig. 6:** Top: Light path in fiber optics. Red: Meridional beams cross only the optical fiber axis. Green: Skew rays do not cross the fiber axis. Middle: Skew rays from a parallel incoming beam. Because of the finite extent of the laser beam, so-called skew rays are generated in different directions, leaving the fiber into different directions depending on the number of internal reflections [4]. Bottom: Light distribution with respect to focal ratio degradation for fibers with different surface roughness of 245nm rms (left) and 8nm rms (right). Incoming angle  $\theta = 8^\circ$ ,  $\lambda = 6330 \text{ \AA}$  [5]. The sharpness of the light ring depends on the surface roughness of the fiber apertures.

## 2. Photometric shift and scrambling

Grating diffraction depends on the respective angle of incidence. For that reason, any angle of incidence of stellar light into the telescope aperture in dispersion direction also affects the position of the spectrum in the dispersion direction. Since the seeing disk at the telescope focus is subject to movements by seeing or tracking errors, the stochastic position and thus wavelength changes limit the accuracy of any spectral measurement to a few meters per second. This is a non-negligible effect for high-precision measurements of radial velocities. Given the symmetric light distribution after the passage of a collimated light beam through a fiber (figure 6) one would assume that the location information is completely lost at the fiber output and photometric offsets are thus fully compensated.

However, this is not the case; the effect is true also for observations with fiber optics. On the other hand, optical fibers have the property to minimize this displacement. This is called "photometric scrambling". We consider the displacement of the stellar image  $d$  in relation to the aperture of the fiber optic  $D$  as well as the relation between the corresponding shift of the PSF in the form of an emission line  $s$  and its  $FWHM$ . The ratio of these two relations is referred to as scrambling gain (figure 7).

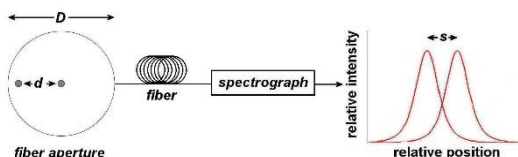


Fig. 7: Photometric shift.

It indicates the stability of the spectral resolution element in relation to the geometric variations of the stellar image at the fiber input aperture. The larger  $G$  the more accurate are the measurements.

$$G = \frac{d/D}{s/FWHM}$$

Avila et al. [4] showed that the spectral accuracy  $G$  can dramatically be increased by simple means. According to their investigations, a non-bent, three-meter-long 60 micron fiber optic cable, which is illuminated by a 50 micron light beam of  $f/2.5$  has a scrambling gain of 120. If this fiber is bent so that the FRD increases by 20%, the scrambling gain increases to 500. The effect is even more dramatic for a non-bent, three-meter-long 600 micron fiber, which is illuminated by a 250 micron beam at  $f/3$ . For this case, a continuous bending of 15mm radius causes a scrambling increase of 150 to 3000. Hence, when the fiber is subject of moderate stress, the spectral measurement accuracy increases by a factor of about 20!

A close examination of scrambling and its gain, respectively, for different fiber cross-sections

has been performed by Avila et al. [6]. They point out that the number of fiber modes depends on both the square of the fiber diameter  $D$  and the numerical aperture  $NA$ .

$$n = \frac{1}{2} \left( \frac{\pi \cdot NA \cdot D}{\lambda} \right)^2$$

Therefore, thicker fibers with a larger  $NA$  provide a more uniform light distribution at the fiber output and the scrambling efficiency should grow. And indeed, the measurements seem to confirm this aspect. However, at least for a round fiber, the  $F$ -number at the input fiber has no influence on the scrambling gain. It is known that mechanical stress causes light loss by increased FRD. Above we already described the possibility to mechanically "shake out" modes and thus improve the achievable spectral S/N. Interestingly, one can also increase the scrambling gain by stress, i.e. by squeezing the fiber (this in turn by increased FRD). In their summary Avila et al. [6] pointed out that circular fibers deliver the highest scrambling gain if they have a large  $NA$  with large diameters and if they are as long as possible. It is then advantageous to squeeze the fiber as they describe it in their text.

## References

- [1] Grupp, F., 2003, Astronomy & Astrophysics, 412, 897
- [2] Sharma, A.B., Halme, S.J. & Butusow, M.M., 1981, Optical Fibre Systems and Their Components, Springer
- [3] Waldschläger, U., 2014, private communication
- [4] Avila, G., Guirao, C., 2009, Tapered optical fibres, <http://spectroscopy.wordpress.com>
- [5] Haynes, D.M., Withford, M.J., Dawes, J.M., Haynes, R., Bland-Hawthorn, J., 2008, SPIE Conference Proceedings, Advanced Optical and Mechanical Technologies in Telescopes and Instrumentation, Eli Atad-Ettedgui; Dietrich Lemke (Eds.) Vol. 7018, p. 8
- [6] Avila, G., Singh, P., Chazelas, B., 2010, SPIE Conference Proceedings, Ground Based and Airborne Instrumentation for Astronomy III, Vol. 7735, p. 1

## **Termine**

**Nicht vergessen / Don't miss:**

### ***ASpekt 14 – Jahrestagung der Fachgruppe 2014***

**ASpekt 14 – Annual Conference of Section Group 2014**

Wann/When: 16. - 18. Mai 2014

Wo/Where: Köln / Cologne

Tagungs- und Gästehaus St. Georg im Zentrum der Kölner Südstadt

***Aktuelle Informationen & Anmeldung /  
Detailed information & registration:***

**[www.spektralklasse.de](http://www.spektralklasse.de)**

### ***Neuer Anfänger Kurs / New Beginner course***

mit Instrukteur / with instructor: Dr. Lothar Schanne

Wann/When: 31. Oktober - 2. November 2014

Wo/Where: Starkenburgsternwarte Heppenheim

***Aktuelle Informationen & Anmeldung /  
Detailed information & registration:***

**[spektroskopie.fg-vds.de](http://spektroskopie.fg-vds.de)**

Diese Seite steht nur Mitgliedern zur Verfügung.

This page is restricted for members only.

**Werden Sie Mitglied in der Fachgruppe Spektroskopie!**  
Mehr Informationen sind beim Fachgruppensprecher erhältlich.

**Become a member of the section group for spectroscopy!**  
Detailed information are available on request. Contact the speaker.

Besuchen Sie / Visit:

**[spektroskopie.fg-vds.de](http://spektroskopie.fg-vds.de)**